

Spontaneous Potential and Electrical Resistivity Response Modelling for a Thick Conductor

¹Adeyemi, A.A., ²A.I. Idornigie and ¹M.O. Olorunfemi

¹Department of Geology, Obafemi Awolowo University, Ile-Ife, Nigeria.

²Department of Geology and Mining, University of Jos, Jos, Nigeria.

Abstract: Direct laboratory modeling of the spontaneous potential (SP) and electrical resistivity responses of a thick conductor with different attitudes was carried out. The aim of the investigation was to obtain characteristic signatures that may be diagnostic of similar geological targets. The method of investigation involved the burial of the conductor at different angles of inclination in sand within a model tank. Measurements were then taken across the conductor and the obtained data were used to generate profiles. The profiles were then interpreted both qualitatively and semi-quantitatively. The results indicate that, on the one hand, SP profiles delineate the conductor better giving the location, information on the magnitude and direction of inclination, and quantitative estimation of the depth of burial. The resistivity profiles, on the other hand, roughly indicated the direction of inclination and location of the conductor. The study concludes that the SP method is suitable for the investigation of sheet-like targets of different attitude, since the results are amenable to both quantitative and qualitative interpretations.

Key words: Modeling, spontaneous potential, electrical resistivity, conductor

INTRODUCTION

Model studies in the discipline of Applied Geophysics have become a very important tool in the interpretation of geophysical data. Electrical modeling studies involve the generation of electrical responses over regular objects (2D or 3D), which are buried in a medium with contrasting physical properties. The use of models in electrical methods of prospecting such as spontaneous potential and electrical resistivity, though not as common as in electromagnetic method^[1], is a useful aid in interpretation of electrical responses over bodies of different shapes, sizes and dimensions^[2]. The natural potential methods (gravity and magnetics) and the electromagnetic methods are areas that have attracted much research using geometric models. Spheres, cylinders, sheets and slabs of different orientations have been used to simulate dykes, faults, anticlines, etc.^[3,4,5]. A successful model experiment helps in better understanding of field signatures over target bodies.

One of the earliest works carried out on the resistivity methods involved a study of apparent resistivity signatures using theoretical models and^[6,7], also documented a very extensive bibliography of resistivity interpretation applicable in mineral investigation and^[8] investigated laboratory responses over a thin conducting dyke and have summarized the various advantages of different electrode arrays in delineating such structure. Theoretical profiles have also been generated over

polarized rods, sheets, slabs and buried spheres using the resistivity techniques^[9]. Contaminant plumes have also been mapped using model studies^[10].

Studies on the interpretation of self-potential anomalies using various geometric models have been carried out^[11,12,13]. Resistivity profiling over a resistive linear structure was achieved by^[14].

Another area of significant research has been the adaptation of theoretical models for computer programs. Iterative modeling using the resistivity and self-potential methods is now made possible by high-speed modern computers and^[15] generated two computer programs important in resistivity prospecting while and^[16] also generated a computer program to calculate self-potential anomalies near vertical dykes.

In this research work, spontaneous potential and electrical resistivity laboratory responses were generated for a thick metallic plate. This conductor simulates a mineralized dyke, a mineralized faulted zone or a mineralized geologic contact that are of interest in mineral investigation. The research work is aimed at improving on the qualitative interpretations of spontaneous potential and electrical resistivity responses for specific configuration of conductive source bodies likely to be encountered on the field (e.g., a mineralized dyke). An attempt is also made at giving a quantitative interpretation that might be generally applicable to conductive targets analogous to the model used, which are often encountered in mineral exploration campaigns.

MATERIALS AND METHODS

A model tank of dimension 117x70x60 cm³ (Fig. 1) was constructed from wooden planks and its interior was lined with transparent cellophane. The tank was filled with sieved river valley sand and then saturated

with water. The set-up was left for 7 hours to establish equilibrium condition within the system. The cellophane helped in preventing loss of saturating fluid in the course of the experiment.

A wall effect test was subsequently carried out to determine areas that are not affected by the anomalously

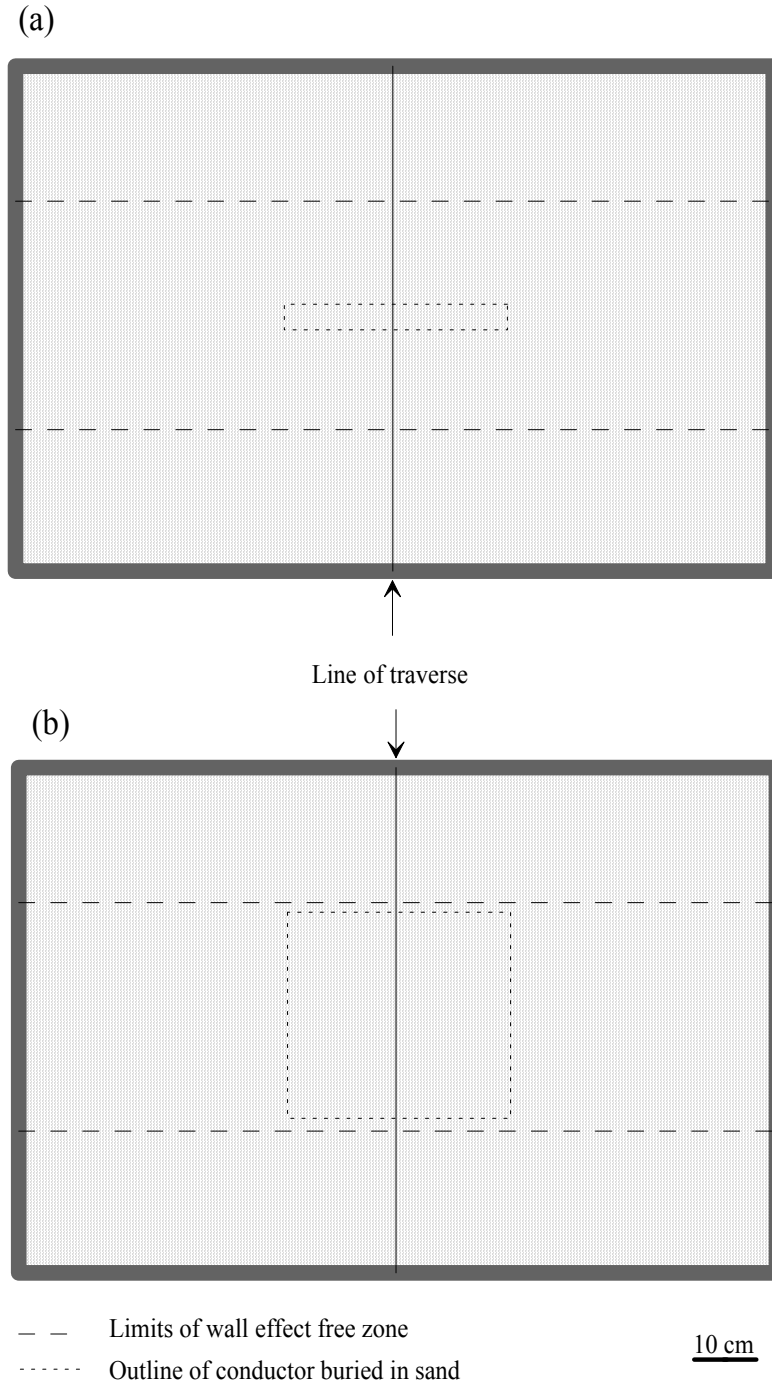


Fig. 1: Plan view of the experimental layout showing the sand-filled wooden tank and the buried conductor with (a) vertical and (b) horizontal disposition

high resistivity values of tank walls. A metal plate of length 34 cm, width 30 cm and thickness 2.6 cm was buried in the sand within the area free of wall effect at a depth (z) of 1.5 cm or 1.75 cm. The inclination of the plate was determined with the aid of a clinometer. In order to ensure that the copper electrodes (length 20 cm and diameter 2 mm) were firmly planted in the sand along a traverse, a wooden plank drilled with holes of 2 mm diameter at regular interval of 1 cm was used as the electrode mount. SP and electrical resistivity measurements were then made with the digital ABEM SAS300C terrameter across the traverse in the wall-effect free zone.

The SP data were acquired with the total field and the gradient arrays (a = 1, 2 and 4 cm) over the conductor inclined at 0°, 30°, 60° and 90°. In all cases, inline profiling was adopted along the traverse. The potentials were plotted against position of the leading electrode P₂ in the total field array, while they were plotted against the midpoint of the pair of electrodes (P₁ and P₂) in the gradient array to generate profiles.

For the different inclinations as enumerated above, electrical resistivity data were acquired using Wenner array with interelectrode separation, a of 2 cm and pole-pole array with interelectrode separation, a of 1 cm. The resistance measured in each case was converted to apparent resistivity values by multiplying with the appropriate geometric factor. The apparent resistivity values were plotted against distance to obtain the required profiles.

The following precautions were observed in the course of data acquisition:

- Good reproducible contact between the copper electrodes and the sand was established while taking measurements.
- The copper electrodes were maintained in a vertical position to ensure a point source of current is delivered in the subsurface.
- The depth of burial of electrodes was the same for all electrodes used.
- In the course of the experiment, spurious values were retaken and were suspected to be due to inadequate contact between sand and electrodes.

RESULTS AND DISCUSSIONS

Spontaneous potential responses:

Total field array response: The SP profiles for the total field array response over the conductor inclined at 0°, 30°, 60° and 90° are shown in Fig. 2, 3, 4 and 5 respectively. The only significant feature of Fig. 2 is that a flat conductor is defined by multiple lows and a central high at the middle. The anomalies for the 30° and 60° inclinations are asymmetrical with a peak minimum. The conductive target dips in the direction of asymmetry, and the top of the conductor coincides with the inflexion points on the anomalies. For the 90° inclination the anomaly is approximately symmetrical with the top of the peak negative anomaly coinciding with the location of the top of the target.

The responses over the conductor inclined at 30°, 60° and 90° were interpreted semi-quantitatively. In order to obtain the depth of burial of the conductor from the profiles, it was observed that the half width rule holds. Half-width is half the width of an anomaly at half the maximum or minimum value^[17]. By rule of thumb

$$x_{1/2} \approx \sqrt{3}.z \tag{1}$$

where $x_{1/2}$ is the half width of the anomaly and z is the depth of burial the conductor. The percent error (%error) in each depth estimate was calculated by using the formula

$$\%error = \frac{Z_{(calculated)} - Z}{Z}.100 \tag{2}$$

where $z_{(calculated)}$ is the depth estimated from the half-width rule. The magnitudes of the values of %error estimated seem to decrease with increase in the angle of inclination (Table 1).

For the asymmetric anomalies for the conductor inclined at 30° and 60°, a tangent to the curve at the maximum curvature of the shoulder on the up-dip side makes an angle θ with the abscissa which is

Table 1: Self potential total field array parameters

Inclination of Conductor	$X_{1/2}$ (cm)	Depth of Conductor, z (cm)	Calculated depth of Conductor, z (cm)	% error	Tangent angle on abscissa, θ
0°	*	1.5	*	*	*
30°	2.83	1.5	1.63	+8.7	≈ 30°
60°	3.0	1.75	1.73	-1.14	≈ 60°
90°	2.64	1.5	1.524	+1.6	*

* Indeterminable

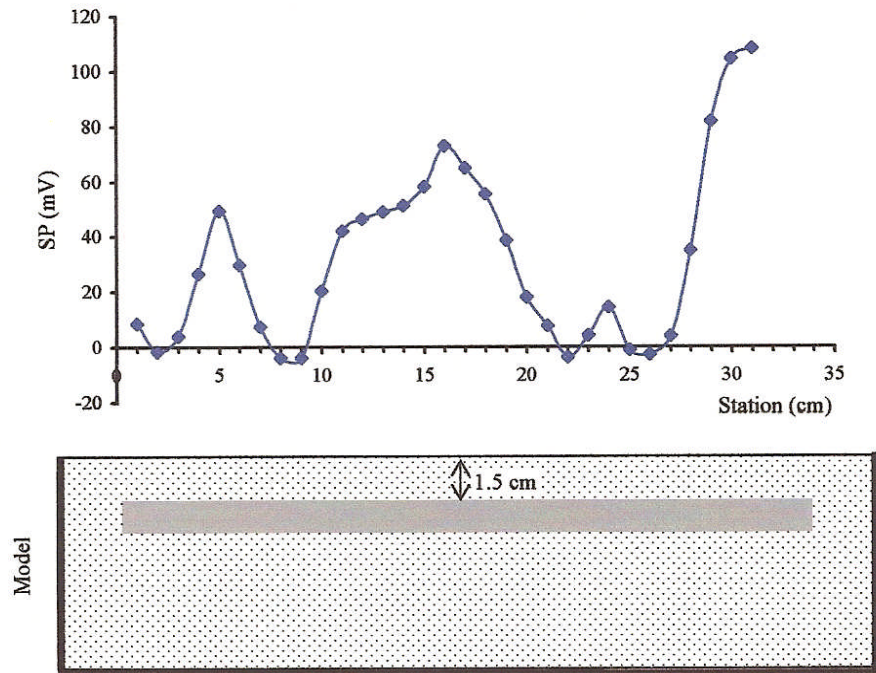


Fig. 2: Self-potential total field array profile over a flat conductor

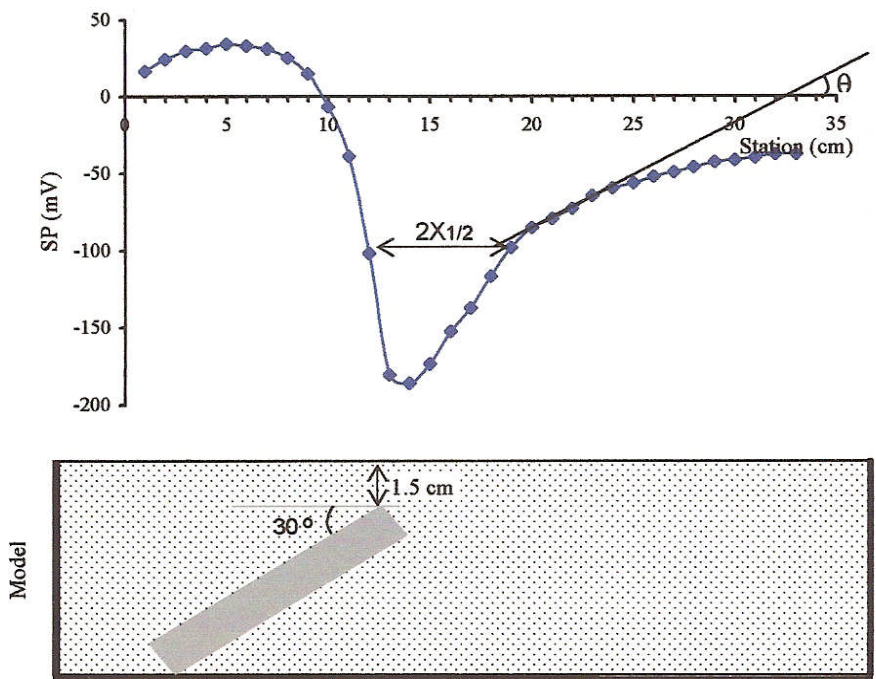


Fig. 3: Self-potential total field array profile over a conductor inclined at 30 degrees to the horizontal

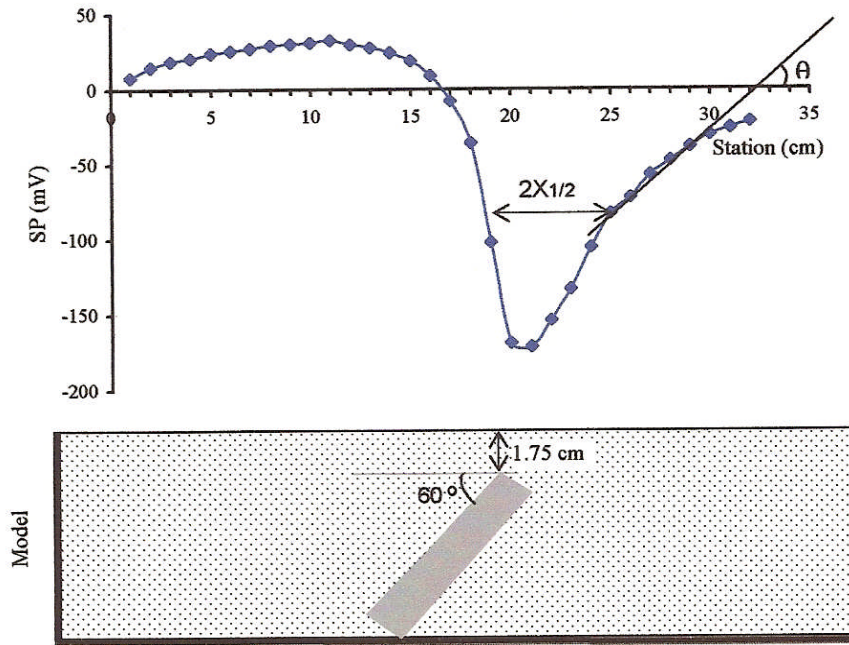


Fig. 4: Self-potential total field array profile over a conductor inclined at 60 degree to the horizontal

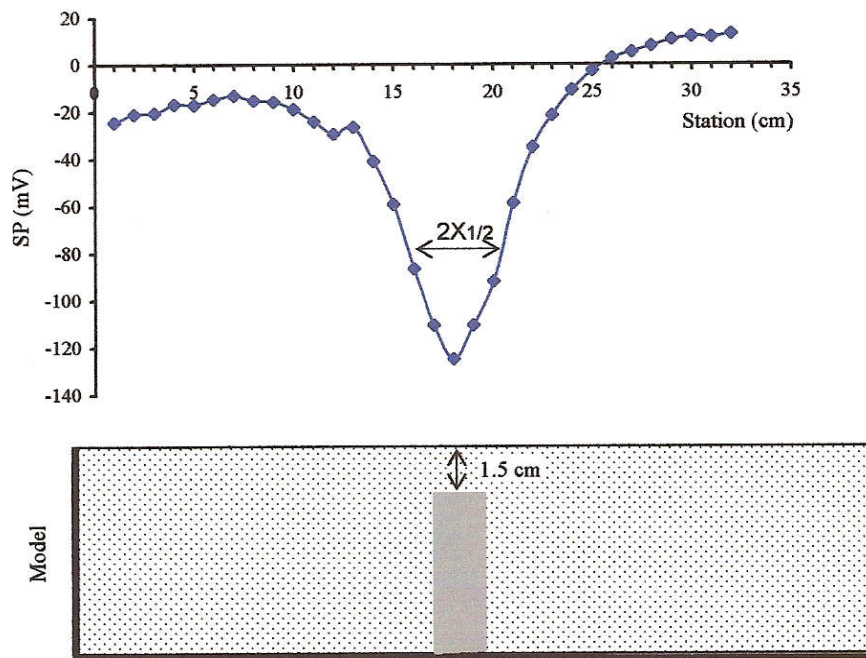


Fig. 5: Self-potential total field array profile over a conductor inclined at 90 degrees to the horizontal

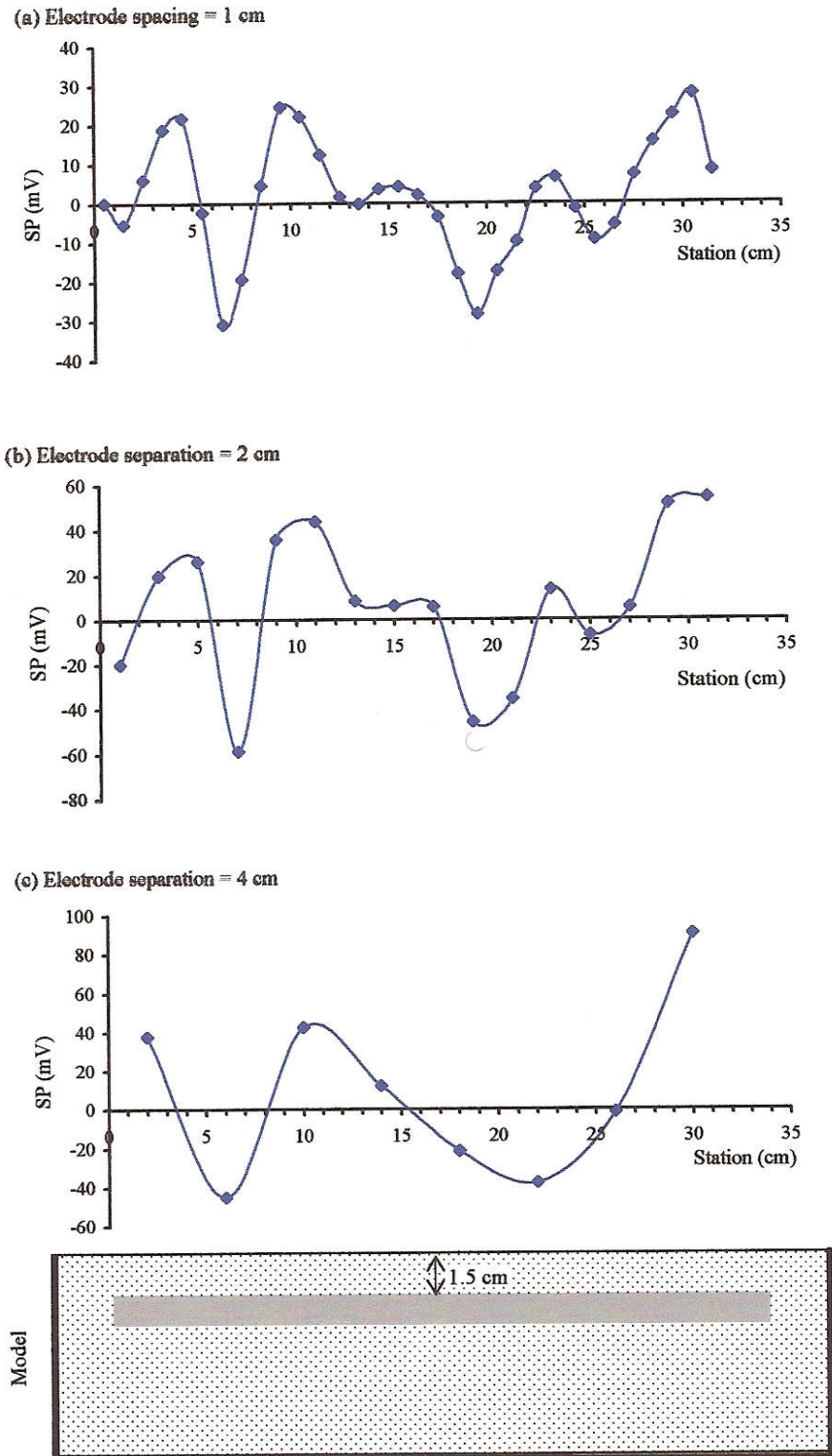


Fig. 6: Self-potential gradient array profiles at different electrode spacing over a flat conductor

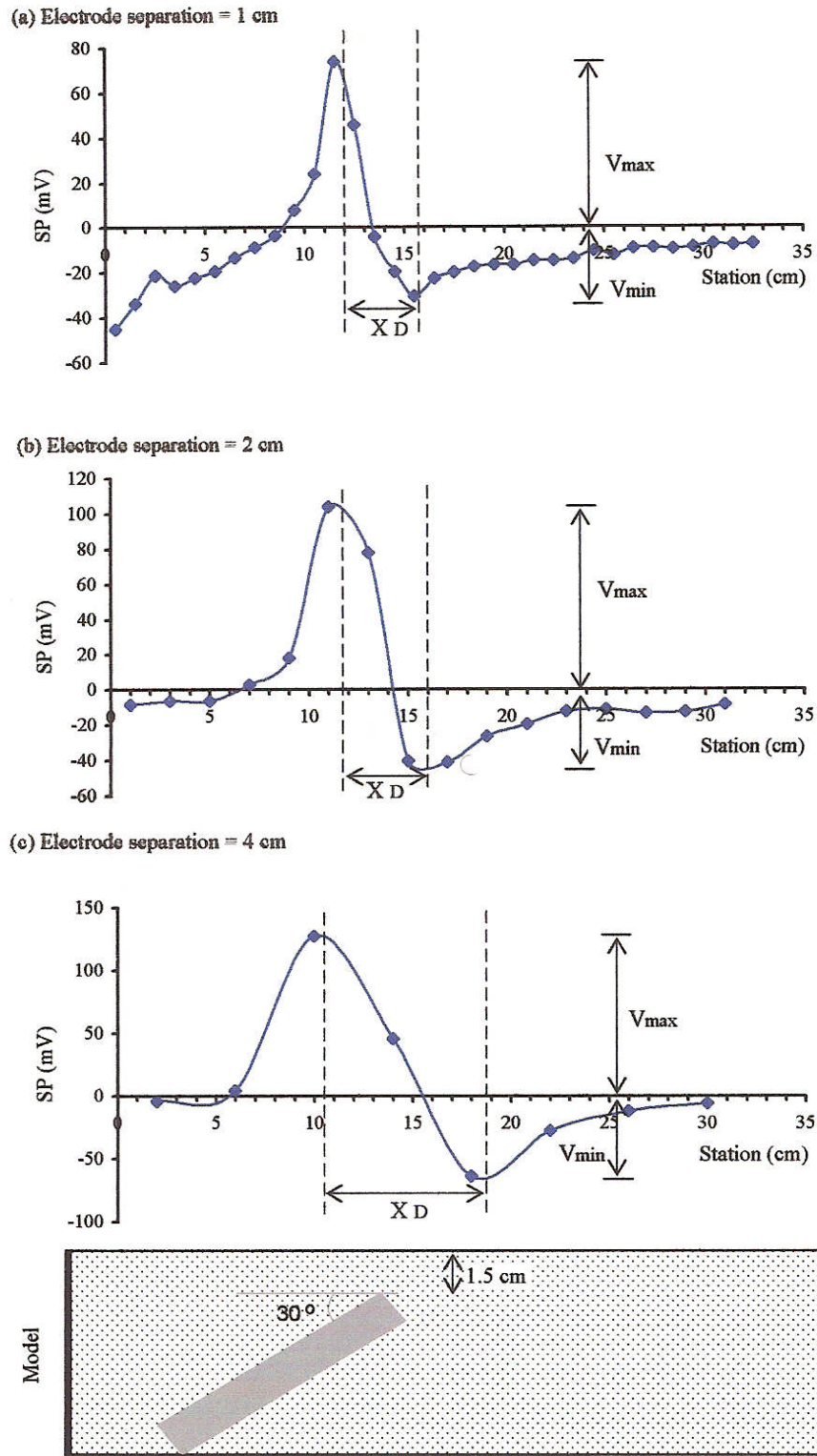
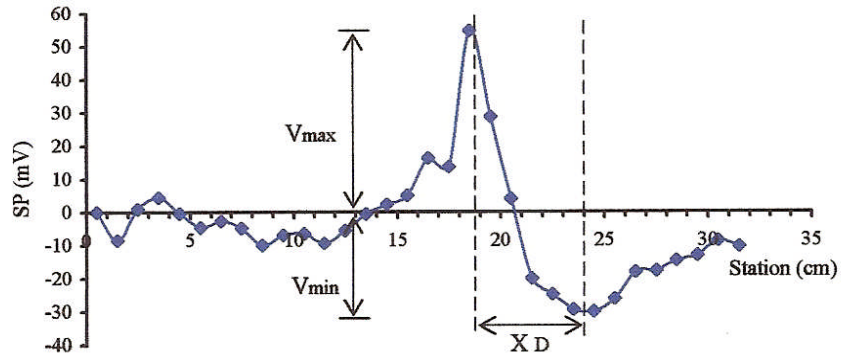
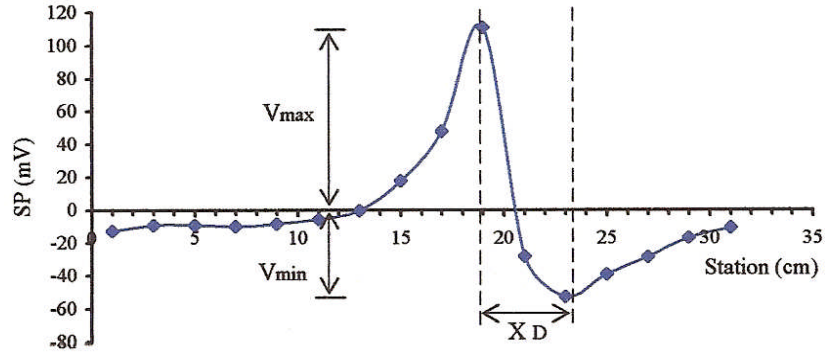


Fig. 7: Self-potential gradient array profiles at different electrode spacing over a conductor inclined at 30 degrees to the horizontal

(a) Electrode separation = 1 cm



(b) Electrode separation = 2 cm



(c) Electrode separation = 4 cm

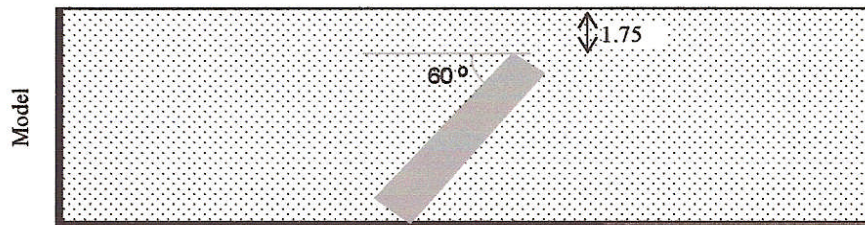
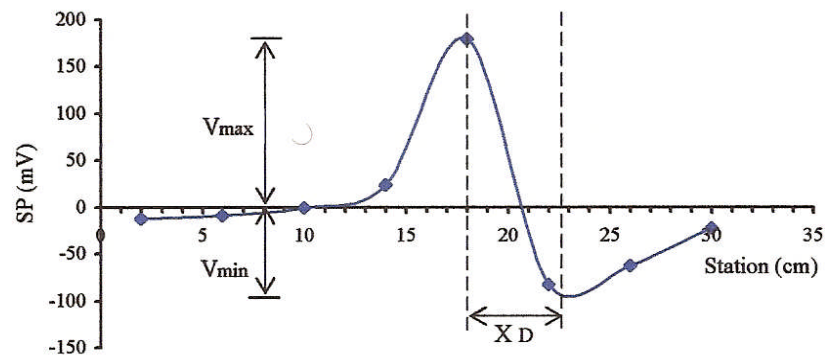


Fig. 8: Self-potential gradient array profiles at different electrode spacing over a conductor inclined at 60 degrees to the horizontal

Table 2: Self potential gradient array parameters

Inclination of Conductor	Electrode Separation (cm)	X_D	Depth of Conductor, z (cm)	Calculated depth of Conductor, z (cm)	%error	$V_{max}/V_{min}>3$
0°	1	*	1.5	*	*	*
	2	*	1.5	*	*	*
	4	*	1.5	*	*	*
30°	1	3.915	1.5	1.503	+0.2	3.2>3
	2	4.67	1.5	1.64	+9.5	3.2>3
	4	5.16	1.5	*	*	*
60°	1	5.62	1.75	1.801	+2.9	2.91<3
	2	4.63	1.75	1.635	-6.6	2.78<3
	4	5.05	1.75	1.71	-2.2	2.5<3
90°	1	3.88	1.5	1.497	-0.2	*
	2	3.92	1.5	1.504	+0.29	*
	4	5.16	1.5	*	*	*

* Indeterminable

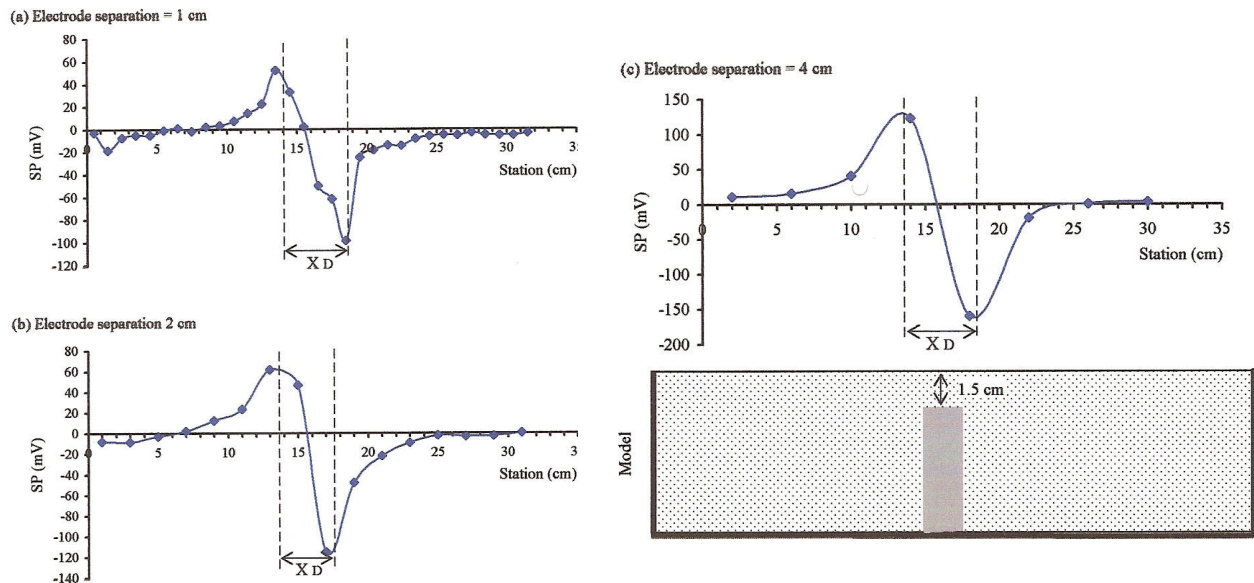


Fig. 9: Self-potential gradient array profiles at different electrode spacing over a conductor inclined at 90 degrees to the horizontal

approximately equal to the inclination angle (Fig. 3 and 4). Table 1 summarizes the results of the semi-quantitative interpretations.

Gradient array response: The gradient array responses show typical sinuous curves (Fig. 6-9). The anomaly for the flat conductor (Fig. 6) does not show any diagnostic feature, but the anomalies for the 30° and 60°

and 90° inclinations have peak positive (V_{max}) and peak negative (V_{min}) amplitudes. The curve is asymmetrical for the 30° and 60° inclinations with the peak positive amplitude established over the down-dip side of the conductor (Fig. 7 and 8), while the curve for the 90° inclination is symmetrical (Fig. 9). In Figures 7-9 the inflexion points of the anomalies give the location of the top of conductor.

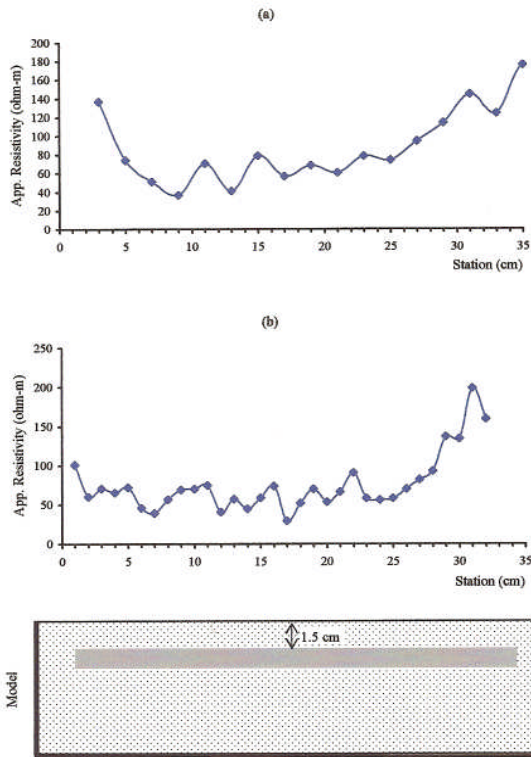


Fig. 10: (a) Werrerr array and (b) pole-pole array profiles over a flat conductor

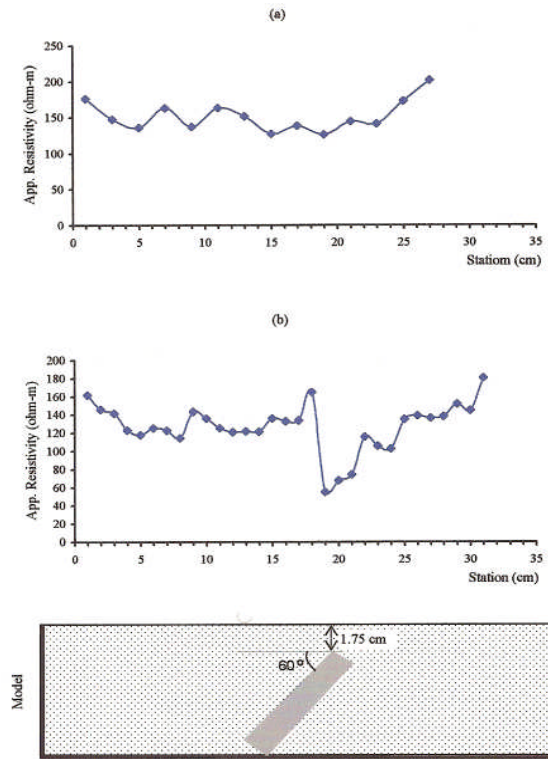


Fig. 12: (a) Werrerr array and (b) pole-pole array profiles over a conductor inclined at 60 degrees to the horizontal

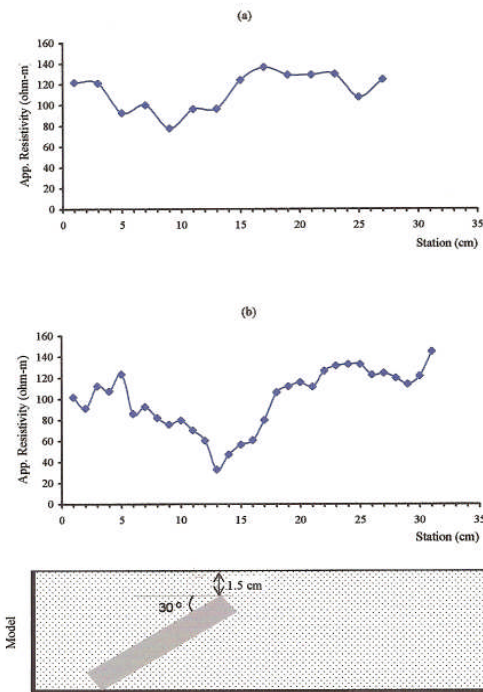


Fig. 11: (a) Werrerr array and (b) pole-pole array profiles over a conductor inclined at 30 degrees to the horizontal

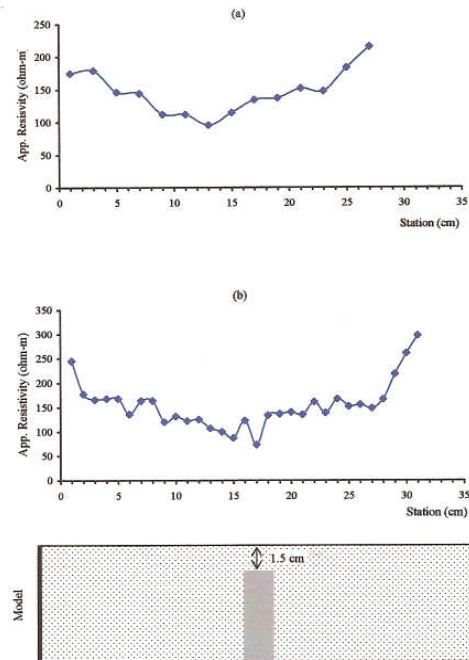


Fig. 13: (a) Werrerr array and (b) pole-pole array profiles over a conductor inclined at 90 degrees to the horizontal

The response of the flat conductor is not susceptible to quantitative interpretation. On the contrary, the gradient array responses have been interpreted semi-quantitatively for orientations of 30°, 60° and 90° to obtain depth to the top of the target z . It has been established that the following rule of thumb holds in this connection

$$x_D \approx \sqrt{3} \cdot z^2 \quad (3)$$

where x_D is the horizontal distance between the peak positive and the peak negative amplitudes. The estimated depths and the corresponding estimation accuracy determined using Equation 2 are shown in Table 2.

The V_{\max} and the V_{\min} ratio was determined to be generally >3, <3 and ≈ 1 for 30°, 60° and 90° inclination cases, respectively (Table 2).

Electrical resistivity responses

Wenner array profiles: The Wenner array apparent resistivity profiles for orientations 0°, 30°, 60°, and 90° are shown in Fig. 10a, 11a, 12a and 13a respectively. Generally, the resistivity lows on the profiles indicate the areas underlain by the conductor. The profile for the 0° inclination does not show any special signature, but that for the 30° inclination shows an approximate S-shape that is symmetrical about the location of the top of the target, which dips in the direction of lower amplitude. At 60° inclination this shape is distorted into a curve with multiple peaks. The point of minimum amplitude coincides with the location of the top of the conductor in the case of 90° inclination.

Pole-pole array profiles: Figure 10b, 11b, 12b and 13b represent the resistivity profiles for the pole-pole electrode array. Like in the case of Wenner array profiles, apart from the generally low resistivity values over the areas underlain by the conductor, the 0° inclination profiles does not indicate any significant feature (Fig. 10b). For the 30°, 60° and 90° inclinations (Figures 11b-13b), the conductor is better delineated compared to the Wenner case. In all these profiles, the resistivity lowest points coincide with the conductor location.

Conclusions: Laboratory model responses over a thick conductor have been generated using SP (total field and gradient arrays) and electrical resistivity (Wenner and pole-pole arrays) methods. The responses were recorded over the conductor buried at depth of 1.5-1.75 cm within sand in a model tank. Records were taken with the conductor inclines at 0°, 30°, 60° and 90° to the horizontal. The recorded data were presented in the form of profiles. The SP profiles were interpreted qualitatively and semi-quantitatively, while the resistivity profiles were

interpreted qualitatively. Visual inspection was used for all the qualitative interpretation, whereas the semi-quantitative interpretation involved the use of empirical relationships derived by rule of thumb.

Results indicate that SP profiles delineate the conductor better giving the location, information on the magnitude and direction of inclination, and quantitative estimation of the depth of burial. The obtained results were within allowable limits of experimental error for both the gradient array and total field array responses. The responses were generally diagnostic of the target. The resistivity profiles also roughly indicated the direction of inclination and location of the conductor. The pole-pole array profiles were more diagnostic compared with the Wenner array profiles.

By way of conclusion, the SP method is suitable for the investigation of sheet-like targets of different attitudes. This is because the results are amenable to both quantitative and qualitative interpretations.

REFERENCES

1. Grant, F.S. and G.F. West, 1968. Interpretation theory in applied geophysics. McGraw-Hill Book Co.
2. Coggon, J.H., 1971. Electromagnetic and electrical modeling by the finite element method. *Geophysics*, 36: 132-155.
3. Geldart, L.P., D.E. Gill and B. Sharma, 1966. Gravity anomalies of 2-D faults. *Geophysics*, 31: 372-97.
4. Telford, W.M., R.E. Sheriff and L.P. Geldart, 1990. Applied geophysics, 2nd ed. Cambridge University Press.
5. Lowrie, W., 1997. Fundamentals of geophysics. Cambridge University Press.
6. Hummel, J.N., 1932. A theoretical study of apparent resistivity in surface potential methods. *Geophysical Prospecting*, 97: 392-427.
7. Van Nostrand, R.G. and K.L. Cook, 1966. Interpretation of resistivity data. U.S.G.S. Professional Paper No. 499.
8. Apparao, A. and A. Roy, 1971. Resistivity modeling experiments II. *Geoexploration*, 9: 195-205.
9. Dey, A. and H.F. Morrison, 1979. Resistivity modeling for arbitrary shaped 3-D structures. *Geophysics*, 44: 753-80.
10. Buselli, G., C. Barber, G.B. Davis, and R.B. Salama, 1990. Detection of groundwater contamination near waste disposal sites with transient electromagnetic and electrical methods. In: S.H. Ward, (Ed.), *Geotechnical and Environmental Geophysics (Investigations in Geophysics, No. 5)*, Vol. 2, Society of Exploration Geophysicists, pp. 27-39.
11. Petrovski, A., 1928. The problem of a hidden polarized sphere. *Phil. and Mag.*, 5: 334-353.

12. De Witte, L., 1948. A new method of interpretation of self-potential field data. *Geophysics*, 13: 600-608.
13. Yungul, S., 1950. Interpretation of spontaneous potential anomalies caused by spherical ore bodies. *Geophysics*, 15: 237-246.
14. Olorunfemi, M.O. and D. Balogun, 1989. A note on resistivity profiling over a resistive linear structure. *Afr. J. Sci. and Tech., Series B-1*, 3: 56-60.
15. Argelo, S.M., 1967. Two computer programmes for the calculation of standard graphs for resistivity prospecting. *Geophysical Prospecting*, 15: 71-79.
16. Fitterman, D.V., 1982. Computer program SPDIKE for calculation of self-potential anomalies near vertical dikes. US Geological Survey Open file Report 82-476.
17. Sheriff, R.E., 1991. *Encyclopedic dictionary of exploration geophysics*, 3rd edition. Geophysical References Series 1, Soc. Expl. Geophysicists.